# Controlling the Critical Current Anisotropy of YBCO Superconducting Films by Incorporating Hybrid Artificial Pinning Centers

Alok K. Jha, Kaname Matsumoto, Tomoya Horide, Shrikant Saini, Paolo Mele, Ataru Ichinose, Yutaka Yoshida, and Satoshi Awaji

***Abstract*—$BaSnO_3$ (BSO) nanocolumns and $Y_2BaCuO_5$ (Y211) nanoparticles have been successfully incorporated into YBCO thin films by premixed and surface modified target approach. The effect of these artificially incorporated nanostructures on the vortex pinning properties of YBCO films is investigated on the basis of variation of critical current density ($J_C$) with applied magnetic field and also its variation with respect to the orientation of the applied magnetic field at two different temperatures: 77 K and 65 K. The incorporation of Y211 nanoparticles in both YBCO and YBCO+BSO2% films results in improved $J_C$-$H$ characteristics which is reflected in the enhanced pinning force density ($F_p$) values. The angular dependent $J_C$ measurement reveals that the YBCO film containing BSO nanocolumns exhibits $J_C$ peak along the *c*-axis, whereas the film containing Y211 nanoparticles exhibits isotropic enhancement in the $J_C$ values along the entire investigated angular regime. The YBCO film consisting of both kinds of nanostructures (BSO nanocolumns together with Y211 nanoparticles), on the other hand, exhibits mixed characteristics of different kinds of pinning: strong *c*-axis $J_C$ peak together with isotropically enhanced $J_C$ in the intermediate angular regime. A possible vortex pinning mechanism due to different kinds of artificially incorporated nanostructures is also discussed.**

*Keywords*— YBCO, thin film, hybrid APCs, vortex pinning

## I. Introduction

THIN FILMS of $YBa_2Cu_3O_{7-\delta}$ (YBCO) superconductor with enhanced critical current density ($J_C$) and reduced anisotropy over wide range of temperature and applied magnetic fields are strongly desired for widespread technological applications [1], [2]. Many efforts have been made in recent years to improve the flux pinning properties of YBCO thin films and majority of these efforts aimed to incorporate nanostructures of secondary phase materials into YBCO superconducting film matrix which generate artificial pinning centers (APCs). The nanostructures of several materials such as $YBa_2CuO_5$ [3], $Y_2O_3$ [4], $BaSnO_3$ [5], [6], $BaZrO_3$ [7], [8], $YBaNbO_6$ [9], [10], etc. have been successfully incorporated into YBCO films which resulted in the enhanced vortex pinning properties of YBCO films deposited by pulsed laser deposition (PLD) technique. Self-assembled nanocolumns of secondary phase materials such as $BaSnO_3$ (BSO), $BaZrO_3$ (BZO), $YBaTaO_6$ (YBTO) *etc.* have resulted in the improvement of $J_C$ values particularly when the applied magnetic field is along the *c*-axis. However, it is strongly desired to improve the $J_C$ performance when the magnetic field is oriented along the intermediate angular regime (between *ab* plane and *c*-axis) as well. In a recent report, it has been shown that the incorporation of hybrid structures (BSO nanocolumns together with $Y_2O_3$ nanoparticles) into YBCO thin film reduces the $J_C$ anisotropy significantly [11].

In the present manuscript, the microstructural and transport properties of YBCO thin films incorporating 1-D APCs (BSO nanocolumns), 3-D APCs (Y211 nanoparticles) and hybrid APCs (BSO nanocolumns + Y211 nanoparticles) is studied. To introduce 1-D and 3-D APCs into the YBCO films, pre-mixed target as well as surface modified targets have been used in the present study. Angular variation of $J_C$ is presented at two different conditions: 77 K, 1 T and 65 K, 3 T which exhibits strongly enhanced critical current densities of the nanocomposite films along broad angular regime. The objective of the present manuscript is to investigate the vortex pinning properties of YBCO film consisting of such hybrid APCs.

## II. Experimental Details

Thin films of YBCO and its nanocomposites with BSO, Y211 and BSO+Y211 have been deposited on single crystal $SrTiO_3$ (STO) substrates using PLD technique (KrF excimer laser, $\lambda$ = 248 nm). The deposition conditions have been described elsewhere [10]. For the deposition of pure YBCO thin film, a pristine YBCO target has been ablated for 9,000 laser pulses. For YBCO+BSO nanocomposite films,

This work was supported by KAKENHI, Grant-in-Aid for Science Research (S), Grant Number 23226014.

A.K. Jha, K. Matsumoto and T. Horide are with Department of Materials Science and Engineering, Kyushu Institute of Technology, Tobata-ku, Kitakyushu 804-8550, JAPAN (e-mail: akjha@post.matsc.kyutech.ac.jp; matsu@post.matsc.kyutech.ac.jp; horide@post.matsc.kyutech.ac.jp) Phone: +81-80-3984-7120

S. Saini was with Institute for Sustainable Science and Development, Hiroshima University, Higashi-Hiroshima 739-8530, JAPAN. He is now with Department of Materials Science and Engineering, University of Utah, Salt Lake City, UT 84112, USA (email: shrikantjnu@gmail.com)

P. Mele is with Materials Science Research Unit, Muroran Institute of Technology, Muroran 050-8585, JAPAN (email: pmele@mmm.muroran-it.ac.jp)

A. Ichinose is with Central Research Institute of Electrical Power Industry, Yokosuka, Kanagawa 240-0196, JAPAN (email: ai@criepi.denken.or.jp)

Y. Yoshida is with Department of Energy Engineering and Science, Nagoya University, Nagoya 464-8063 JAPAN (email: yoshida@nuee.nagoya-u.ac.jp)

S. Awaji is with Institute for Materials Research, Tohoku University, Sendai 980-8577 JAPAN (email: awaji@imr.tohoku.ac.jp)

YBCO+BSO(2%) pre-mixed target was used in which BSO content is 2% by weight. For YBCO+Y211 and YBCO+BSO+Y211 films, the surface of the same YBCO and YBCO+BSO targets are modified by a sticking a thin rectangular Y211 pieces (3.6 area %) on the top of the targets by means of silver paste. As the target is rotated, the Y211 portion is periodically ablated allowing the formation of Y211 nanoparticles in the YBCO and YBCO+BSO films. Two of the samples: YBCO and YBCO+BSO2% have already been studied in our previous work [11]. The microstructure of YBCO+Y211 and YBCO+BSO+Y211 nanocomposite films have been studied using transmission electron microscopy (TEM). Transport properties of these thin film samples have been measured using four-probe method by a Physical Property Measurement System (PPMS, Quantum Design). A voltage criterion of 1 $\mu Vcm^{-1}$ has been used to obtain the critical current values. Angular dependence of $J_C$ of all the thin film samples was measured at 77 K, 1 T and 65 K, 3 T using the same voltage criterion.

## III. RESULTS AND DISCUSSION

The cross-sectional transmission electron micrographs of YBCO+Y211 and YBCO+BSO2%+Y211 films have been presented in Fig. 1(a), (b) and (c), (d) respectively at different magnifications. The formation of Y211 nanoparticles in all the images and that of the BSO nanocolumns in Fig. 1 (c) and (d) can be observed clearly. The formation of some planar defects is also observed which are usually generated during the growth of the film and has been reported earlier also [10]. Using both mixed target and surface modified target approach; both nanoparticles and nanocolumns are incorporated in the YBCO film matrix.

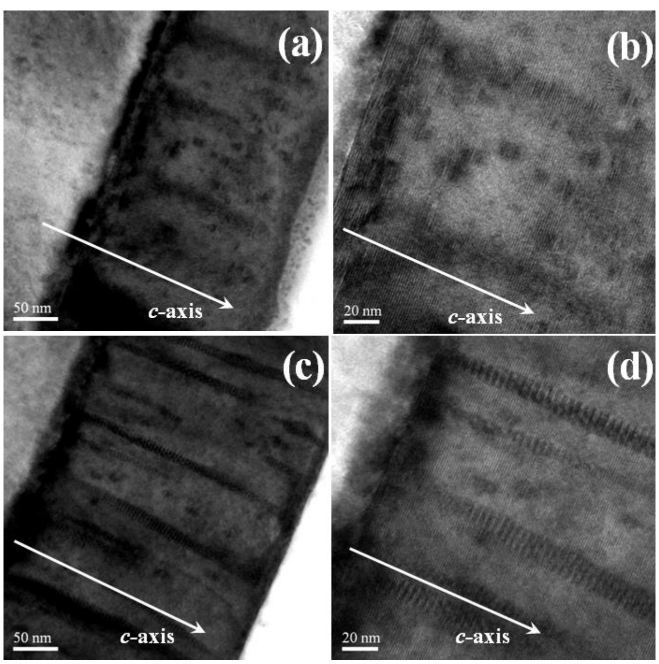


**FIG. 1 Cross-sectional transmission electron micrographs of YBCO+Y211 film (a), (b) and YBCO+BSO2%+Y211 film (c), (d) at different magnifications. The formation of nanoparticles in both the cases and that of nanocolumns in sample with hybrid APCs can be observed.**

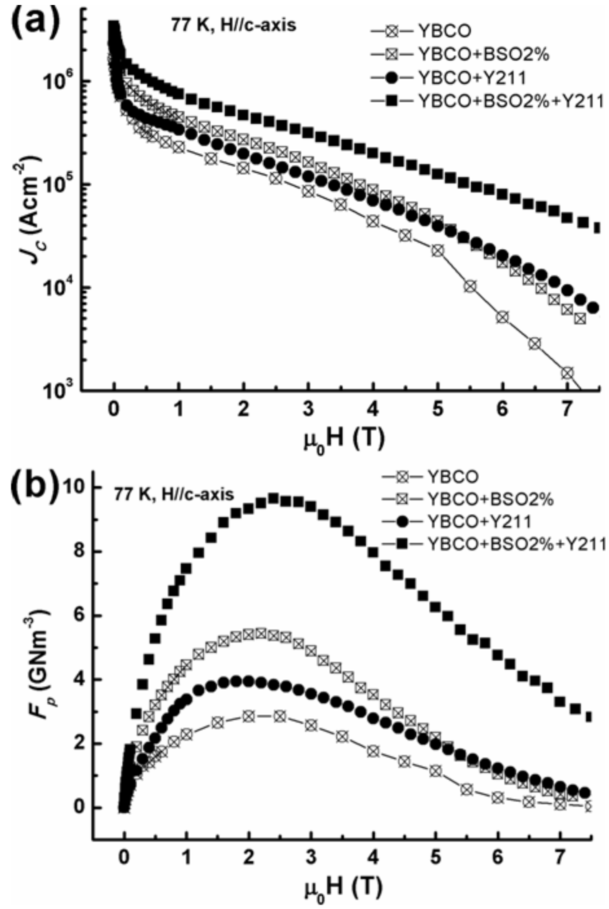


**FIG. 2 Variation of $J_C$ (a) and $F_P$ (b) with applied magnetic field for YBCO, YBCO+BSO2%, YBCO+Y211 and YBCO+BSO2%+Y211 at 77 K.**

The variations of $J_C$ and $F_p$ with applied magnetic field for all the studied thin film samples at 77 K are presented in Fig. 2. The self-field $J_C$ values of all the studied samples vary between 1.6-3.4 $MAcm^{-2}$. The $J_C$-$H$ characteristics of YBCO+BSO nanocomposite film is improved as compared to that of pure YBCO film. YBCO+Y211 film also exhibits improved $J_C$-$H$ characteristics as compared to the pure YBCO film but inferior to the YBCO+BSO film. However at sufficiently higher field (~ 5T), YBCO+Y211 film starts overtaking the YBCO+BSO film, although the enhancement is not significant. YBCO+BSO+Y211 film, on the other hand, exhibits significantly improved $J_C$-$H$ characteristics and this improvement is more prominent at higher applied magnetic field. The improved $J_C$-$H$ characteristics are also reflected in the $F_p$-$H$ plot. With incorporation of Y211 nanoparticles, both YBCO and YBCO+BSO films exhibit higher $F_{pmax}$ values. At 77 K, $F_{pmax}$ for YBCO film is 2.86 $GNm^{-3}$ whereas it increases to 3.95, 5.44, and 9.65 $GNm^{-3}$ for YBCO+Y211, YBCO+BSO2% and YBCO+BSO2%+Y211 films respectively. The improvement in the $J_C$-$B$ characteristics is more prominent at 65 K which is shown in Fig. 3. At 65 K, $F_{pmax}$ for YBCO film is 13.6 $GNm^{-3}$ whereas it increases to 31.57, 36.08, and 44.70 $GNm^{-3}$ for YBCO+Y211, YBCO+BSO2% and YBCO+BSO2%+Y211 films respectively.

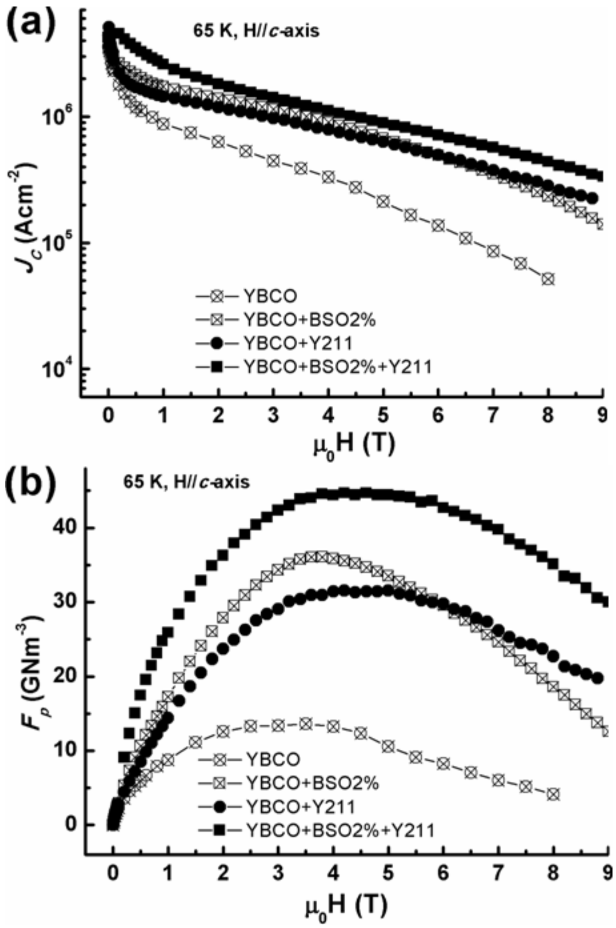


**FIG. 3 Variation of $J_C$ (a) and $F_p$ (b) with applied magnetic field for YBCO, YBCO+BSO2%, YBCO+Y211 and YBCO+BSO2%+Y211 at 65 K.**

There is significant increase in the $F_{pmax}$ values of the nanocomposite films consisting of APCs indicating the effectiveness of both BSO nanocolumns and Y211 nanoparticles as strong pinning centers. The incorporation of Y211 nanoparticles in both YBCO and YBCO+BSO films leads to the shifting of the $\mu_0 H_{max}$ (the applied magnetic field at which $F_{pmax}$ occurs) towards higher values and it is more prominent at 65 K. At 65 K, $\mu_0 H_{max}$ for YBCO, YBCO+Y211, YBCO+BSO2% and YBCO+BSO2%+Y211 films are 3.5, 4.2, 3.8 and 4.6 T respectively which means that pinning is more effective at higher applied magnetic field in films consisting of hybrid APCs. Shifting of $\mu_0 H_{max}$ towards higher applied magnetic field can be understood in terms of the nanorod and vortex densities in the samples. Usually, vortices occupy the nanorods (correlated disorder along the *c*-axis) as long as the applied magnetic field is less than or equal to the matching field. However, as the applied magnetic field keeps on increasing, the nanorods cannot accommodate any more vortices and here the nanoparticles start pinning the vortices as random pinning centers at places between the nanorods. Thus pinning force is provided by both the nanorods and the nanoparticles in the samples consisting of the hybrid APCs. The nanoparticles can also act differently: they can prevent the vortex motion in the case of double-kink formations as a consequence of thermal activations as suggested by Maiorov *et al.* [12].

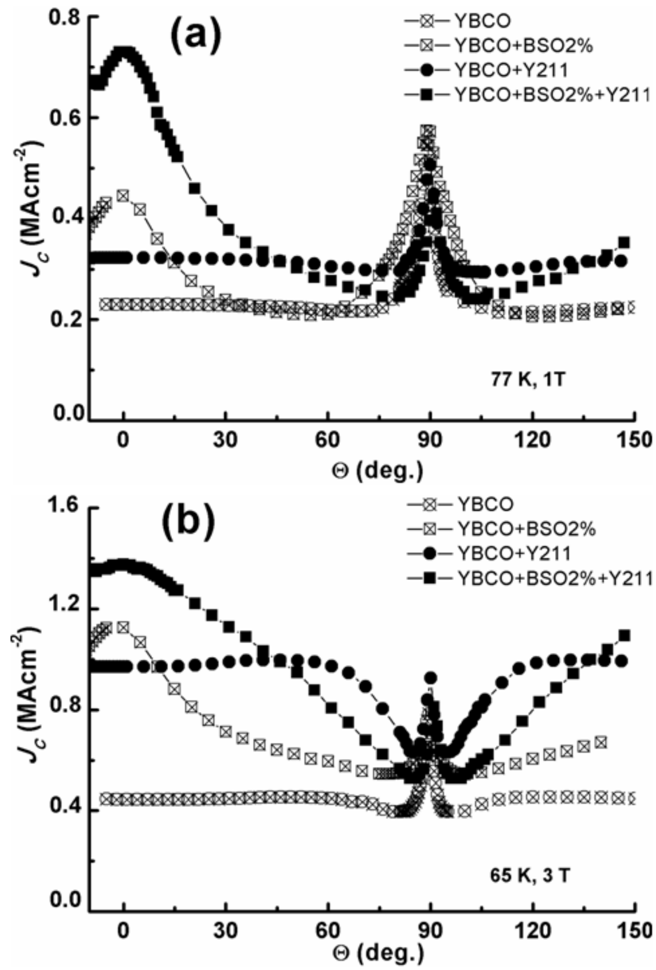


**FIG. 4 Angular dependence of $J_C$ for YBCO, YBCO+BSO2%, YBCO+Y211 and YBCO+BSO2%+Y211 at (a) 77 K, 1 T and (b) 65 K, 3T.**

Fig. 4 shows the angular dependence of $J_C$ for all the 4 thin films measured at two different conditions: (a) 77 K, 1 T and (b) 65 K, 3 T. The improved angular dependent $J_C$ behavior can be clearly observed in the YBCO+BSO2% nanocomposite film where strong enhancement in the *c*-axis direction is due to continuous BSO nanocolumns. The angular variation of YBCO+211 film, however, exhibits uniform enhancement of $J_C$ along the entire investigated angular regime at both the temperatures. However, at 65 K, this enhancement is more prominent. Uniform $J_C$ along the entire angular regime (except the angular regime near to ab plane) is an evidence of the isotropic pinning provided by the Y211 nanoparticles. Similar observation has been made by Viswanathan *et al.* [13], in which uniform enhancement in $J_C$ was achieved through incorporation of $Y_2O_3$ nanoparticulates. The samples consisting of hybrid APCs exhibit enhanced $J_C$ values not only along the *c*-axis but also along the intermediate angular regime at both the temperatures due to cooperative contributions of both 1-D and 3-D APCs. At 77 K, 1 T (Fig. 4(a)), the incorporation of only BSO nanocolumns resulted in 2-fold increase in the $J_C$ value along the *c*-axis which is the consequence of strong pinning of vortices by BSO nanocolumns. However, as the Y211 nanoparticles are further incorporated into it, the *c*-axis peak becomes even more pronounced. This is a bit unusual as the BSO nanocolumns concentration in both the films are expected to be the same. It is, however, possible, that the additional Y211 nanoparticles, which are randomly distributed, restrict the motion of the double-kink segments of the vortices which are formed as a result of thermal activations thus preventing further dissipation. In the pristine YBCO film the strong $J_C$ peak along the ab-plane is observed because of its layered structure where the weak superconducting layers provide stability to the flux lines when these are parallel to the *ab*-plane [14]. Apart from this intrinsic pinning provided by the weak superconducting layers, it is also expected that the planar defects, which are generated during the growth of the film, contribute to vortex pinning significantly particularly when the magnetic field is along the *ab*-plane [15]. In the hybrid APCs sample, BSO nanocolumns are expected to provide *c*-axis pinning and Y211 providing isotropic pinning. However, $J_C$ enhancement is gradually decreasing from the *c*-axis to the *ab*-plane before becoming minimum at $\theta = 80°$.

The reduction of $J_C$ by changing the applied magnetic field orientation has been described by Paulius *et al.* [16]. According to their model, when the inclination of the magnetic field with respect to *c*-axis increases, the length of the trapped portion of the vortex decreases and subsequently $J_C$ becomes low. At sufficient inclination, no region of the vortex is trapped and $J_C$ becomes minimum. In the present case of samples consisting of hybrid APCs, even though the vortices can become free of the BSO columnar disorders in the intermediate angular regime, the Y211 nanoparticles can pin different portions of the vortices irrespective of the orientation of the applied magnetic field which results in the improved $J_C$ values along all the magnetic field orientations. It, therefore, can be concluded that the combination of 1D+3D APCs is very useful in improving the vortex pinning properties of YBCO films which can be observed in terms of increased $F_{pmax.}$ values, shifting of $\mu_0 H_{max}$ towards higher applied magnetic fields and improvement of $J_C$ values along all the orientations of the applied magnetic field.

## IV. CONCLUSIONS

Columnar (1-D) as well as spherical (3-D) APCs have been successfully incorporated into YBCO film matrix. $F_{pmax}$ and $\mu_0 H_{max}$ values got enhanced significantly by incorporating the Y211 nanoparticles in both pure YBCO and YBCO+BSO films which has been attributed to the strong pinning of vortices by Y211 nanoparticles. The angular dependence of $J_C$ exhibited significant improvement in the YBCO film with hybrid APCs not only along the *c*-axis but also along the intermediate angular regime. The variation of the proportion of 1-D APCs (BSO nanocolumns) and 3-D APCs (Y211 nanoparticles) in YBCO film matrix is expected to provide even better critical current properties with reduced anisotropy.

## V. ACKNOWLEDGEMENT

This work was supported by KAKENHI, Grant-in-Aid for Science Research (S), Grant Number 23226014.

## REFERENCES

[1] S. R. Foltyn, L. Civale, J. L. M. Driscoll, Q. X. Jia, B. Maiorov, H. Wang, and M. Maley, "Materials science challenges for high-temperature superconducting wire," Nat. Mater., vol. 6, 631, 2007.

[2] D. C. Larbalestier, A. Gurevich, D. M. Feldmann and A. Polyanskii, High $T_C$ superconducting materials for electric power applications, Nature (London) 414, 368, 2001.

[3] T. Haugan, P. N. Barnes, R. Wheeler, F. Meisenkothen, and M. Sumption, "Addition of nanoparticle dispersions to enhance flux pinning of the $YBa_2Cu_3O_{7-x}$ superconductor," Nature, vol. 430, pp. 867-870, 2004.

[4] P. Mele, K. Matsumoto, T. Horide, A. Ichinose, M. Mukaida, Y. Yoshida, and S. Horii, "Insertion of nanoparticulate artificial pinning centers in $YBa_2Cu_3O_{7-x}$ films by laser ablation of a $Y_2O_3$ surface modified target," Supercond. Sci. Technol., vol. 20, pp. 616-620, 2007.

[5] P. Mele, K. Matsumoto, A. Ichinose, M. Mukaida, Y. Yoshida, S. Horii, and R. Kita, "Systematic study of $BaSnO_3$ insertion effect on the properties of $YBa_2Cu_3O_{7-x}$ films prepared by pulsed laser ablation," Supercond. Sci. Technol., vol. 21, 125017, 2008.

[6] C. V. Varanasi, J. Burke, H. Wang, J. H. Lee, and P. N. Barnes, "Thick $YBa_2Cu_3O_{7-x}$ +$BaSnO_3$ films with enhanced critical current density at high magnetic fields," Appl. Phys. Lett., vol. 93, 092501, 2008.

[7] A. Goyal, S. Kang, K. J. Leonard, P. M. Martin, A. A. Gapud, M. Varela, M. Paranthaman, A. O. Ijaduola, E. D. Specht, J. R. Thompson, D. K. Christen, S. J. Pennycook, and F. A. List, "Irradiation-free, columnar defects comprised of self-assembled nanodots and nanorods resulting in strongly enhnaced flux-pinning in $YBa_2Cu_3O_{7-\delta}$ films," Supercond. Sci. Technol., vol. 18, pp. 1533-1538, 2005.

[8] J. L. M. Driscoll, S. R. Foltyn, Q. X. Jia, H. Wang, A. Serquis, L. Civale, B. Maiorov, M. E. Hawley, M. P. Maley, and D. E. Peterson, "Strongly enhanced current densities in superconducting coated conductors of $YBa_2Cu_3O_{7-x}$ +$BaZrO_3$," Nat. Mater., vol. 3, pp. 439-443, 2004.

[9] D. M. Feldmann, T. G. Holesinger, B. Maiorov, S. R. Foltyn, J. Y. Coulter, and I. Apodaca, "Improved flux pinning in $YBa_2Cu_3O_7$ with nanorods of the double perovskite $Ba_2YNbO_6$," Supercond. Sci. Technol., vol. 23, 095004, 2010.

[10] A. K. Jha, K. Matsumoto, T. Horide, S. Saini, P. Mele, Y. Yoshida, and S. Awaji, "Tuning the microstructure and vortex pinning properties of YBCO based superconducting nanocomposite films by controlling the target rotation speed" Supercond. Sci. Technol., vol. 27, 025009, 2014.

[11] A. K. Jha, K. Matsumoto, T. Horide, S. Saini, P. Mele, A. Ichinose, Y. Yoshida and S. Awaji, "Tailoring the vortex pinning strength of YBCO thin films by systematic incorporation of hybrid artificial pinning centers" Supercond. Sci. Technol., vol. 28, 114004, 2015.

[12] B. Maiorov, S. A. Bailey, H. Zhou, O. Ugurlu, J. A. Kennison, P. C. Dowden, T. G. Holesinger, S. R. Foltyn and L. Civale, "Synergetic combination of different types of defect to optimize pinning landscape using $BaZrO_3$-doped $YBa_2Cu_3O_7$" Nat. Mater., vol. 8, 398, 2009.

[13] S. K. Viswanathan, A. A. Gapud, M. Varela, J. T. Abiade, D. K. Christen, S. J. Pennycook and D. Kumar, "Enhancement of critical current density of $YBa_2Cu_3O_{7-\delta}$ thin films by self-assembly of $Y_2O_3$ nanoparticulates," Thin Solid Films, vol. 515, 6452, 2007.

[14] M. Tachiki, and S. Takahashi, "Anisotropy of critical current in layered oxide superconductors," Sol. St. Comm., vol. 72, pp. 1083-1086, 1989.

[15] H. Yamasaki, K. Ohki, I. Yamaguchi, M. Sohma, W. Kondo, H. Matsui, T. Manabe, and T. Kumagai, "Strong flux pinning due to dislocations associated with stacking faults in $YBa_2Cu_3O_{7-\delta}$ thin films prepared by fluorine-free metal organic deposition," Supercond. Sci. Technol., vol. 23, 105004, 2010.

[16] L. M. Paulius, J. A. Fendrich, W.-K. Kwok, A. E. Koshelev, V. M. Vinokur, G. W. Crabtree, and B. G. Glagola, "Effects of 1-GeV uranium ion irradiation on vortex pinning in single crystals of the high-temperature superconductor $YBa_2Cu_3O_{7-\delta}$," Phys. Rev. B, vol. 56, pp. 913-924, 1997.